Vol. 44, No. 4 (2022) 707-718, DOI: 10.24874/ti.1371.09.22.11

Tribology in Industry

www.tribology.rs

RESEARCH

Design of Experiment with Tribological Performance Analysis of Electroless Nano-composite Ni-P-SiC Coating for Conveyors

Santosh Kumar[a,*], Subrata Kumar Ghosh[b], Nitin Namdeo Pawar[a], Surendra Harichandra Rathod[a], Manoj Ashok Chaudhari[a], Raja Ram Bhagat[a], Rohith Goli[b]

[a]*Department of Mechanical Engineering, Alamuri Ratnmala Institute of Engineering and Technology Shahapur Thane, Mumbai University, India,*
[b]*Department of Mechanical Engineering, Indian Institute of Technology (ISM), Dhanbad, India.*

Keywords:

Electroless coating
Wear
Friction
Optimization
ANOVA

* Corresponding author:

Santosh Kumar
E-mail: santosh.kumar0190@gmail.com

Received: 17 September 2022
Revised: 27 October 2022
Accepted: 16 November 2022

A B S T R A C T

Present study examines friction and wear characteristics for Ni-P-SiC coated SS 304 steel sample and It is used in conveyors in terms of increment in life cycle of conveyors under dry condition with cost effective manner. It is one of the most commonly produced and used stainless steel grades. So, this research is focused on SS304. The surface of SS 304 steel is finished by Ni-P-SiC electroless coating, and its characteristics have been studied through different analyses. FESEM with EDAX has been used to identify the elemental distribution of samples. Taguchi L16 orthogonal array, ANOVA, and regression analysis have been used to obtain experiment layout, significant process parameters, and linear relationship between input and output variables, respectively, under the experiment of design and validate with confirmatory test. Combination of operating parameters which minimize both coefficient of friction and wear is generated using multi-objective optimization. Experiments are carried out according to L16 orthogonal array and the significant parameters among the chosen, which influence wear and coefficient of friction of Ni-P-SiC electroless coated SS 304 under dry conditions are determined. Relations between the output variable and input variable is established by linear regression equations of the friction coefficient between interacting components and wear under the dry condition in terms of load, speed, and temperature. 10 N, 100 rpm, and 90 °C are found to be an optimum set of operating parameters among selected levels which minimize both wear and coefficient of friction of sample.

1. INTRODUCTION

One-fourth of the world's energy demand arises from tribological contacts. Steel finds its suitability in many engineering applications because of its high tensile strength. Apart from such characteristics, specific properties such as tolerance to corrosion and excellent formability

are essential to suit for applications in the field of food processing, pharmaceutical sectors. SS 304 is austenitic stainless steel that exhibits superior corrosion resistance even under exposure to a variety of atmospheric environments and corrosive media, thus suiting best for machinery in the above sectors. Yet again, industrial applications demand enhanced anti-wear and anti-friction characteristics, as in the case of metal conveyor belts used in material handling. Coating technology is one among, which emerged to fulfill those characteristics. Many researchers have investigated different coating techniques and their suitability to varying grades of steel as a substrate to explore the benefits in terms of tribological performance. It examined the frictional characteristics and wear behaviour for plain carbon steel substrates under nickel, chromium deposition and reported that chromium plating provided high wear resistance than an electroless nickel as it forms surface oxide film which is capable of acting as barrier layer but limitation being lower hardness and hot hardness. It was stated that hardness of nickel coating deposited by electroless technique is about twice of the value obtained through electroplating. Electrodeposition was used to form the metal matrix composite coating on steel sample and found the impressive improvement in hardness and corrosion resistance. Efforts were made by several researchers in enhancing the performance under tribological aspects using these techniques [1]. Authors investigated the tribological phenomena considering wear quantitatively and friction for NiP, NiP with PTFE deposited through electroless technique on high-speed steel and concluded that both the coatings resulted in improved wear behaviour whereas significant rise of wear resistance in later is due to PTFE particles incorporation in NiP deposition [2]. It performed WS2 incorporated electroless Ni-P coating on aluminium samples and examined the wear, hardness and corrosion resistance features. It was reported that Ni-P-WS_2 composite coatings provide less friction coefficient inspite of severe sliding condition compared to Ni-P coating. Evolution of nanotechnology and its wide range of applications directed the researchers to focus on the usage of nanoparticles to influence the tribological characteristics of material. Significant work was carried out by them [3]. It examined the result of CNT addition in Ni based coatings on low carbon steel and concluded that Ni-based CNT composite coatings exhibit less friction coefficient and more wear resistance than Ni-P coating [4]. It evaluated the CNT-Ni-P coated medium carbon steel substrates and confirmed that they provide much less rate of wear in comparison with nickel coated substrates and of substrates without coating [5]. It incorporated diamond nanoparticles in electroless Ni-P deposition performed on steel with low content of carbon and stated that it improved corrosion resistance [6]. It produced and analysed the characteristics of Ni-B-SiC deposited by electroless technique on carbon steel and stated that it enhanced the micro-hardness, corrosion resistance and provides uniform surface finish [7]. It examined the resultant characteristics by SiC addition into Ni-P bath solution used in electroless deposited composite coatings deposited on mild steel and concluded that it improves hardness apart from corrosion and wear resistance of substrates compared to Ni-P coatings [8]. It examined extent of contribution of load being applied, distance and velocity of sliding, size of reinforcement particle and CRT glass weight percent on rate of wear and friction coefficient behaviour of magnesium- based hybrid composites [9]. It conducted experimental analysis applying Taguchi methodology principles in orthogonal array to obtain an optimum composition mixture of filler and base material in polyphenylene sulphide composites that provides enhanced tribological performance [10]. It adopted Taguchi technique for analysing influence of speed, pressure and duration on the wear behaviour of PEEK composites [11]. It studied the Inconel 600 alloy wear characteristics by conducting experimental investigation according to Taguchi methodology in which load, speed, sliding distance and pin temperature were selected as input parameters [12]. It carried out multi response optimisation of aluminium matrix composites in which various parameters including sliding speed, sliding distance, load and weight percent of reinforcement being used are set to their optimum level to yield minimum dry frictional coefficient and specific rate of wear [13]. Co–P alloy matrix composite with nano-MoS_2 solid lubricant [14], Ni-P-TiC composite coatings [15], graphene incorporated electroless Ni-P composite coatings [16], electroless Ni-P with TaC composite coating [17], electrodeposited Co-P alloy [18], electroless Ni-P-TiO2 composite [19], electrodeposition of Ni-P/Ni-Co-Al_2O_3 [20], electrodeposition of Co-P coatings reinforced by MoS_2 and Y_2O_3 hybrid ceramic nanoparticles [21] used to improve mechanical and tribological properties.

The morphology of surface was changed and enhanced the corrosion resistance of the coating using Ni-P and nano SiC. The micro-hardness of Ni-P-SiC coating obtained by electroless method was higher than Ni-P coating. It has been found that the SiC superfine particles are uniformly distributed into Ni-P coating [22]. Many authors described the optimal process parameter with Taguchi based Design of Experiment [23-28].

Based on above stated facts, the current analysis focuses on exploration of electroless Ni-P-SiC deposition on wear and friction behavior of SS 304 sample and impact of considered operating parameters on these phenomena of this coated substrate under different sliding conditions is also investigated. Optimum tribological parameters, load, speed and temperature for multiple responses, wear and coefficient of friction for coated substrate can be well determined through optimization by statistical design of experiments. The present study deals with the design of the experiment approach on SiC-Ni-P electroless coated nanocomposite on SS304 with novel work. The detailed microstructure analysis, mechanical testing, and investigation of tribological behaviour were performed for coated and uncoated samples. Taguchi's L16 orthogonal array is used to identify the optimum input processing parameters for minimum wear and lowest CoF. ANOVA (analysis of variance) shows the most significant input parameters. Mathematical model is used to develop the model and establish the strong relationships between input (speed, load and temperature) and output (mass loss and CoF) parameters. The experimental tests verified the proposed model.

2. METHODOLOGY

2.1 Preparation of plating bath

The surface area of each samples is 854.5 mm^2. The bath loading is defined as a total metal area of plates immersed in the solution per bath volume. This parameter should be kept in the range of 0.3-1.5 dm^2/dm^3 for stable plating. The bath loading of electroless coating is approximately 0.42 dm^2/dm^3 for stable plating in experimental analysis. The electroless coating method has been applied on the grind sample [22]. Electroless nickel bath solution composition and its operating conditions are indicated in the Table 1.

Table 1. EN solution components and operating condition.

Solution Composition		
Chemicals		Concentration (g in 300 ml) with 60 minutes heating
Nickel sulphate	Solution 1	6.3
Sodium hypophosphite		7.2
Lactic acid		6.86
Picric acid		0.68
Nano SiC	Solution 2	0.6
CTAB		0.03
Operating Condition		
pH		4.2
Temperature		85-90 ℃

Each of the required constituents are weighed to the exact amount using digital weighing balance and bath solution of 300 ml was prepared. Temperature is observed by dipping the thermometer into the bath. Ni-P coating has been done on the uncoated samples by dipping in the solution 1 for 60 min as shown in Figure 1. The nano SiC with CTAB (cetyl trimethyl ammonium bromide) as surfactant are mixed in bath solution 1 to prepare solution 2. Homogeneous mixing has been done by bath type ultrasonicator (Piezo-U-Sonic, 229C). The pin is dipped again inside solution 2 for 60 minute at 80°C. Figure 2 shows the surface change of sample before coating and after SiC-Ni-P nanocomposite electroless coating [22]. Digital pH meter was utilized to quantify pH of solution. SiC nanoparticles were ultra-sonicated using a bath type ultra sonicator before introducing them into Electroless Nano (EN) coating solution as it results in good dispersion of nanoparticles in the solution.

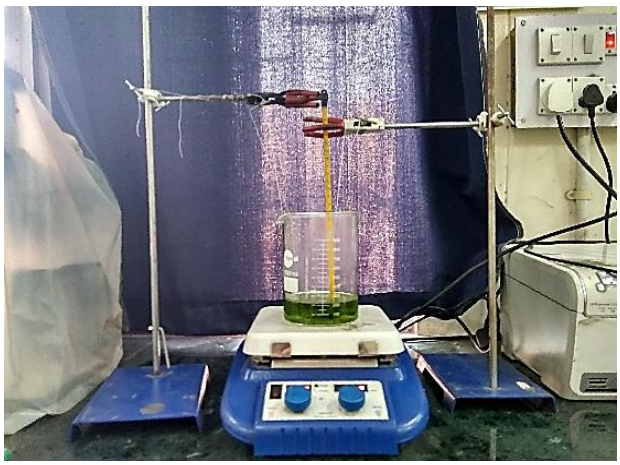

(a) Ni-P solution

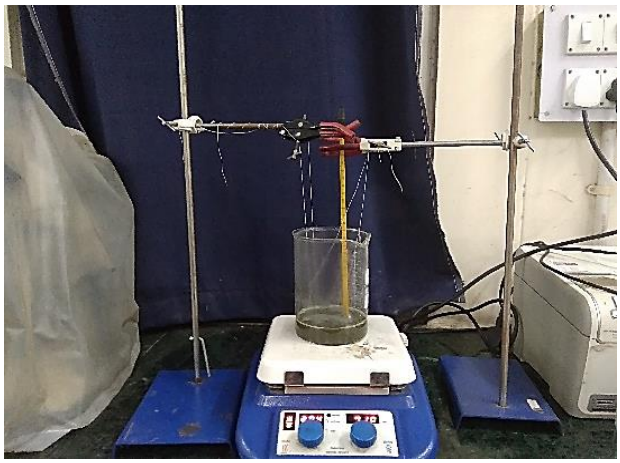

(b) Solution after addition of SiC nanoparticles

Fig. 1. Electroless coating setup.

SS 304 metallic pins of diameter 8 mm and height 20 mm were used as substrates for coating. These are prepared by performing turning operation on round bar of SS 304 and finishing operations were later performed to obtain desired surface roughness. The process involved for sample preparation before coating is as indicated in the Figure 2.

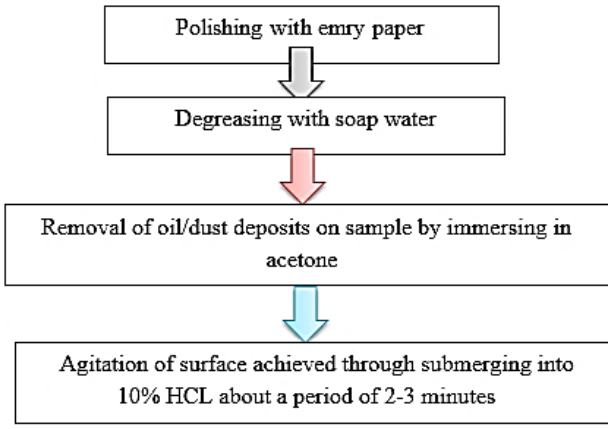

Fig. 2. Flowchart indicating the procedure of sample preparation before coating process.

Now the sample was introduced into the Ni-P solution and placed for about 30 minutes for allowing Ni-P base layer to get coated over the surface. Stir has been done at small at 100 rpm. It is used to prevent the settlement of dissolved particles.

SiC nano particles whose average diameter is 50 nm were added into bath solution and ultrasonicated for 30 minutes to get dispersed in the solution. Ni-P coated sample are immersed in the ultra-sonicated bah solution for about 1.5 hour at desired range of pH and temperature to obtain Ni-P-SiC composite coating.

3. RESULTS AND DISCUSSION

3.1 Surface analysis

Electroless deposition results in uniform coated surface over the substrate. Figure 3 (a)-(b) illustrates the Field Emission Scanning Electron Microscopy (FESEM) image with Energy Dispersive X-Ray Analysis (EDAX) (Carl ZEISS, Sigme2546) of SS 304 surface without coating. It shows that uncoated sample have C, K, Fe, Cu, Al, and Sb and Fe as major elements. and Figure 3 (c)-(d) depicts FESEM image with EDAX of the uniform coated surface of SS 304 achieved through electroless coating. It shows that uncoated sample have C (42 wt.%), Ni (12 wt.%), P (22 wt.%), and Si (24 wt.%). So, this analysis is verified the Ni-P-SiC composite coating on the SS-304 surface. FESEM image shows the coated sample at 15.00 KX magnification have smoother than uncoated sample at 1.00 KX magnification.

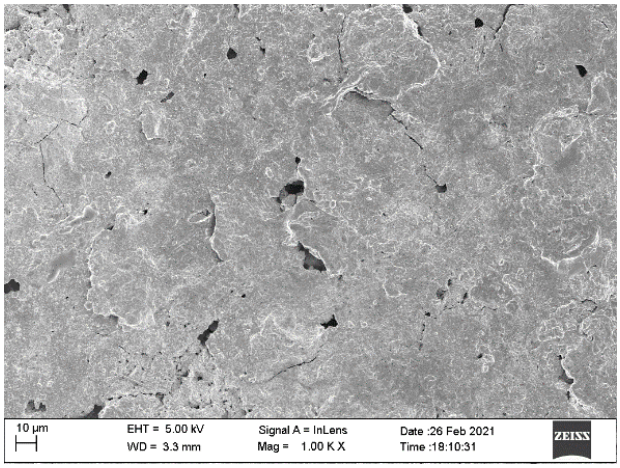

(a) FESEM image of uncoated sample.

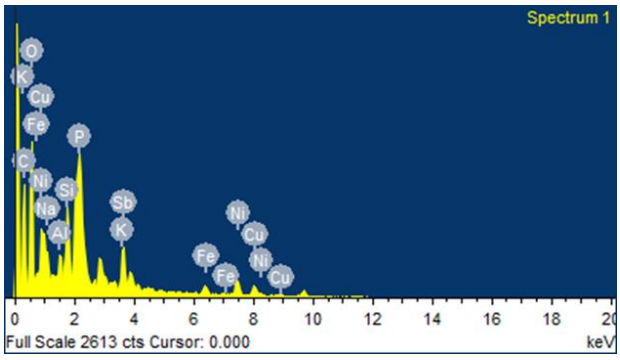

(b) Elemental analysis of uncoated sample

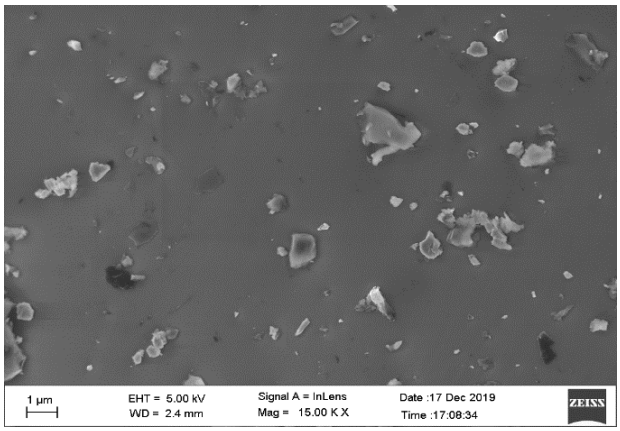

(c) FESEM image of coated sample

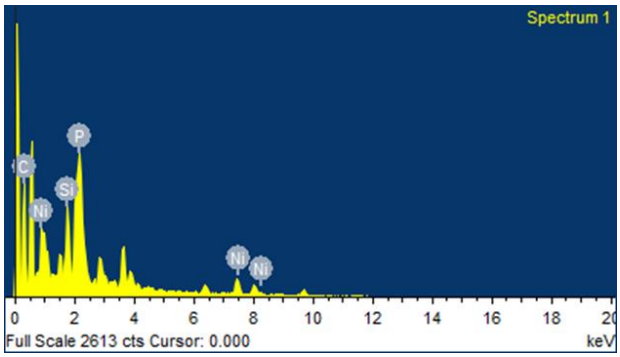

(d) Elemental analysis of coated sample

Fig. 3. FESEM with EDAX analysis of uncoated and coated SS 304 sample surface.

3.1.1 Thickness analysis

Field Emission Scanning Electron Microscopy (FESEM) image (Carl ZEISS, Sigme2546) analysis is used to measure the thickness of coating. It has been observed that the average thickness of coating is 71.862 µm as shown in Figure 4.

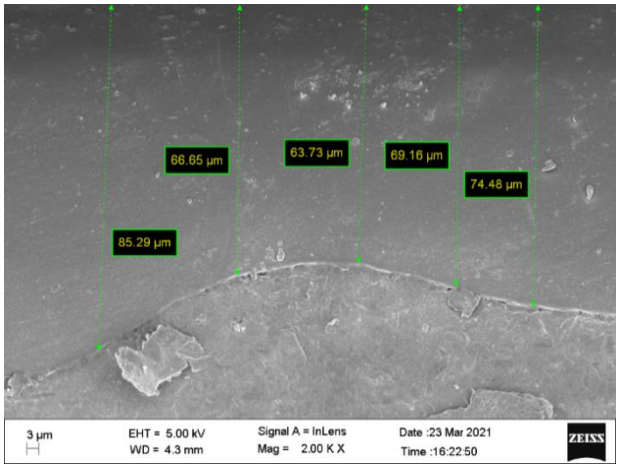

Fig. 4. FESEM cross-sectional image of coated SS-304 sample.

3.1.2 Hardness analysis

Micro hardness of the samples has been measured in a micro hardness tester 'LM 248 AT' (LECO, serial no. XM8 116, Michigan). Average micro-harness value of uncoated sample is 270 HV. Average micro-harness value of uncoated sample is 305 HV.

3.2. Design of experiment

Load, velocity, and temperature are the most prominent factors for wear rate and CoF, and it vary with the change in the morphology of contact surfaces. The literatures reveal that abrasive wear is more dominating factor below the 300 ºC and significant improvement of wear resistance has been observed at high temperature. Tribological performance evaluation: Tribology tests are performed on a Pin-on-disc tribometer (Model: TR201LE, Make: Ducom Devices). Wear and CoF are observed by LVDT (Linear Variable Differential Transformer) and strain gauge load cell sensors. K type thermocouple sensors are utilized to measure temperature rise in brake pad samples [22]. The influence of considered factors over desired output variables is investigated experimentally by applying design of experiments. In present study, Taguchi based design of experiments is adopted thereby minimizing cost and time involved in study. Load, speed and temperature are considered as control factors in which each factor has four chosen levels. The units of process variables are indicated in Table 2. L16 orthogonal array is selected on basis of design of experiments by Taguchi methodology.

Table 2. Levels of process variables.

Control factor	Level 1	Level 2	Level 3	Level 4
Load (N)	10	20	30	40
Speed (rpm)	100	200	300	400
Temperature(°C)	30	60	90	120

3.2.1 Wear analysis

The rate of wear resulted from sixteen experimental runs conducted as per L_{16} orthogonal array are tabulated in Table 3. Signal to noise ratio (S/N) of corresponding test runs are calculated using the equation below for smaller the better characteristic of response variable, wear.

$$\frac{S}{N} = -10\log[\frac{1}{n}(\sum y2)]$$

Where n is the number of observations for a test run and y is the observed value.

Table 3. L_{16} orthogonal array of experiments, observed wear and calculated signal to noise ratio.

Test Runs	Load (N)	Speed (rpm)	Temperature (℃)	Wear (μm)	S/N Ratio
1	10	100	30	6.47	-16.2181
2	10	200	60	9.07	-19.1521
3	10	300	90	8.42	-18.5062
4	10	400	120	10.66	-20.5551
5	20	100	60	13.04	-22.3056
6	20	200	30	16.00	-24.0824
7	20	300	120	14.89	-23.4579
8	20	400	90	12.97	-22.2588
9	30	100	90	22.10	-26.8878
10	30	200	120	22.55	-27.0629
11	30	300	30	20.41	-26.1969
12	30	400	60	24.34	-27.7264
13	40	100	120	30.16	-29.5886
14	40	200	90	33.82	-30.5835
15	40	300	60	35.16	-30.9210
16	40	400	30	38.75	-31.7654

The factor combination of 10 N load, 100 rpm speed and 30°Ctemperature results in minimum wear with maximum value of S/N ratio from experimental observations.

The response analysis of all the factors for the S/N ratio is indicated in Table 4. Order of significance among the selected factors is indicated by rank in S/N ratio response table. Rank 1 indicates it as most significant factor among selected factors whose influence is dominant on response variable. Rank is decided based on the value of Delta. Difference of maximum and minimum mean value of S/N ratio is termed as delta. It is found that the load is the most significant factor for wear of the sample under this study.

Table 4. Signal to noise ratio response table of wear.

Level	Load (N)	Speed (rpm)	Temperature(℃)
1	-18.61	-23.75	-24.57
2	-23.03	-25.22	-25.03
3	-26.97	-24.77	-24.56
4	-30.71	-25.58	-25.17
Delta	12.11	1.83	0.61
Rank	1	2	3

The most significant factor is concluded from plot of signal to noise ratio main effects for wear based on the factor possessing highest slope. Load exhibits the highest slope and it is the dominant factor for wear of sample under study compared to speed and temperature, as shown in Figure 5.

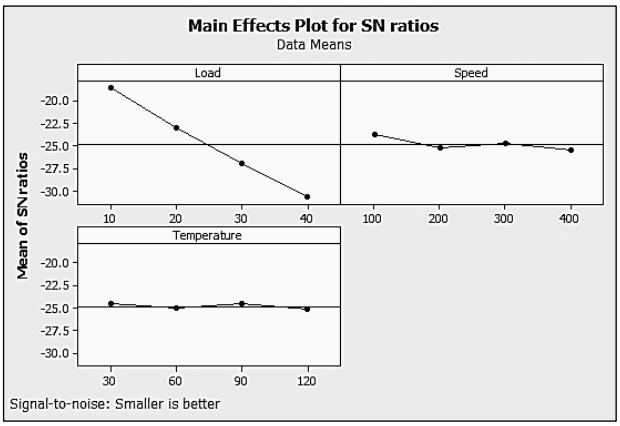

Fig. 5. Plot of signal to noise ratio main effects for wear.

3.2.1.1 Regression model for wear

The amount of sample wear rate corresponding to the governing input variables, load, temperature and speed is predicted by the equation below which is modelled by linear regression analysis. The extent to which the model fits the data is quantified through coefficient of determination, R^2. The wear equation exhibits an adjusted R^2 of 93.66%, indicates that the 93.66% variance in wear rate is predictable from the factors under study, load, speed and temperature. Consistency in the values resulting is good enough as R^2 and its adjusted value, R^2(adj.) exceeded 90%.

$$W = 3.21125 + (0.855775 \cdot \mathrm{L}) + (0.0105725 \cdot \mathrm{S}) - (0.0120083 \cdot \mathrm{T})$$

Figure 6 shows plot of residuals normal probability for wear and depicted that values are close enough to normal probability. The normal distribution is followed by errors is indicative from this plot.

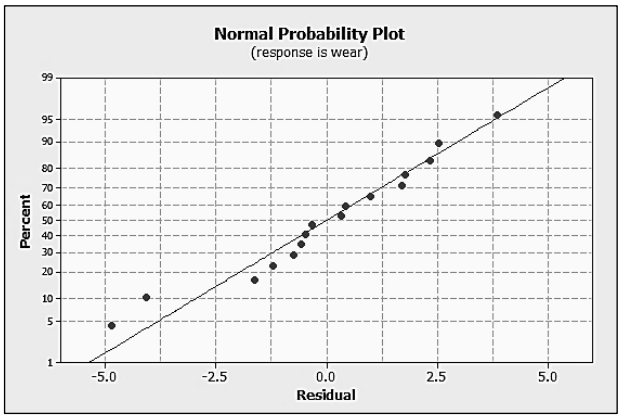

Fig. 6. Plot of residuals normal probability for sample wear.

Results from analysis leads to R^2 and its adjusted value, R^2(adj) as 94.93% and 93.66% respectively for wear as tabulated in Table 5. Different Coefficient (Coef.) is used to defined the mathematical model. Standard Error (SE) Coefficient is an estimation of the standard deviation of the coefficient. The P- values (predictor value) of the load have 0.000. It is less than 0.05. It means that the null hypothesis has been rejected and the alternative hypothesis has been accepted. The load and temperature are more significant parameters to establish the input and output relationship. The P-value for the temperature is 0.543, i.e., it is larger than 0.05. It means that it is an insignificant parameter to contribute to the developing input and output relationship. The suitability of the calculated constants is high as considerably good determination coefficient (R^2) to the tune of 0.9493 is obtained for wear and hence the model is adequate to use for further analysis.

Table 5. Linear regression analysis of sample wear.

Terms	Coef	SE Coef	T	P
Constant	-3.21125	2.57574	-1.2467	0.236
Load	0.85578	0.05760	14.8584	0.000
Speed	0.01057	0.00576	1.8357	0.091
Temperature	-0.01201	0.01920	-0.6255	0.543
S=2.57574	R^2 =94.93%		R^2(adj)=93.66%	

3.2.1.2 Analysis of variance for wear

ANOVA is performed to analyze extent of input variables load, temperature and speed influence on sample wear characteristics. The analysis is carried out at 5% level of significance. Table 6 shows results of this analysis for wear of sample.

The parameters used in Table 6 are expressed in the form of equations (1) to (5) (Kothari, 2004; Roy, 2004; Krishnaiah and Shahabudeen, 2012).

DF of a factor = Number of the level of a factor –1 (1)

DF of the total set of experiments = Total number of results of all trials -1 (2)

The sum of square (SS) is expressed as:

$$\text{Sum of Square (SS)} = \sum_{i=1}^{n}(Y_i - \bar{Y})^2 \quad (3)$$

The value of Adjusted Sum of Square (Adj.SS) is the same as the SS data set.

Adjusted Mean Square Error (Adj.MSE) is expressed in Equation (4) as:

$$\text{Adj. MS or Variance} = \frac{\text{Each factor Adj.SS}}{\text{Each factor DF}} \quad (4)$$

F- value is expressed as:

$$F - ratio = \frac{Adj.MS}{Adj.MSE} \quad (5)$$

Table 6. Sample wear ANOVA results.

Source	DF	Adj SS	Adj MS	F-value	p-value	P%
Load (N)	3	1508.05	502.68	105.99	0.000	96.09
Speed (rpm)	3	28.97	9.66	2.04	0.210	1.85
Temperature (°C)	3	3.79	1.26	0.27	0.848	0.24
Error	6	28.46	4.74			
Total	15	1569.27				

Load has maximum influence (96.09%) whereas other input factors speed (1.85%) and temperature have negligible influence on response variable, wear.

3.2.2 Coefficient of friction analysis

The friction coefficient resulted and corresponding S/N ratio for all sixteen test runs are tabulated in Table 7.

Table 7. L_{16} orthogonal array with experimental results and S/N ratio.

Test Runs	Load (N)	Speed (rpm)	Temperature (°C)	Friction coefficient	Sample S/N Ratio
1	10	100	30	0.07	23.0980
2	10	200	60	0.08	21.9382
3	10	300	90	0.06	24.4370
4	10	400	120	0.05	26.0206
5	20	100	60	0.10	20.0000
6	20	200	30	0.11	19.1721
7	20	300	120	0.13	17.7211
8	20	400	90	0.12	18.4164
9	30	100	90	0.14	17.0774
10	30	200	120	0.15	16.4782
11	30	300	30	0.16	15.9176
12	30	400	60	0.17	15.3910
13	40	100	120	0.18	14.8945
14	40	200	90	0.20	13.9794
15	40	300	60	0.19	14.4249
16	40	400	30	0.21	13.5556

The response analysis of all the factors for S/N ratio is tabulated in Table 8. It is found that the load is most prominent factor for friction coefficient of sample under this study.

Table 8. S/N ratio response table for friction coefficient.

Levels	Load (N)	Speed (rpm)	Temperature (°C)
1	23.87	18.77	17.94
2	18.83	17.89	17.94
3	16.22	18.13	18.48
4	14.21	18.35	18.78
Delta	9.66	0.88	0.84
Rank	1	2	3

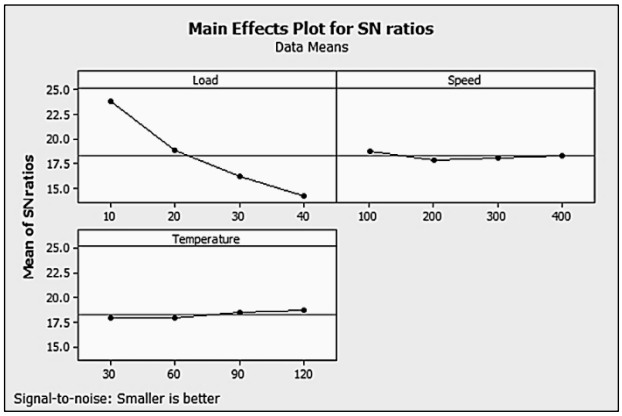

Fig. 7. Plot of main effects for S/N ratio of CoF.

The most significant factor is concluded from plot of main effects of S/N ratio based on the factor possessing highest slope as shown in Figure 7. Load exhibits the highest slope and it is the dominant factor for coefficient of friction of sample under study compared to speed and temperature.

3.2.2.1 Regression model for coefficient of friction

The amount of coefficient of friction of the sample with respect to the governing input variables, load, speed and temperature is predicted by the equation below which is modelled by linear regression analysis. The extent to which the model fits the data is quantified through coefficient of determination, R^2. The coefficient of friction equation exhibits an adjusted R^2 of 96.24%, indicates that the 96.24% variance in friction coefficient is predictable from factors under study, load, speed and temperature. Consistency in the values resulting is good enough as R^2 and its adjusted value, R^2(adj) exceeded 90%.

$$C = 0.0225 + (0.0043 \cdot L) + (4.5e-005 \cdot S) - (0.000116667 \cdot T)$$

Figure 8 is plot of residuals normal probability of friction coefficient indicating that values are close enough to normal probability. The normal distribution is followed by errors is indicative from this plot.

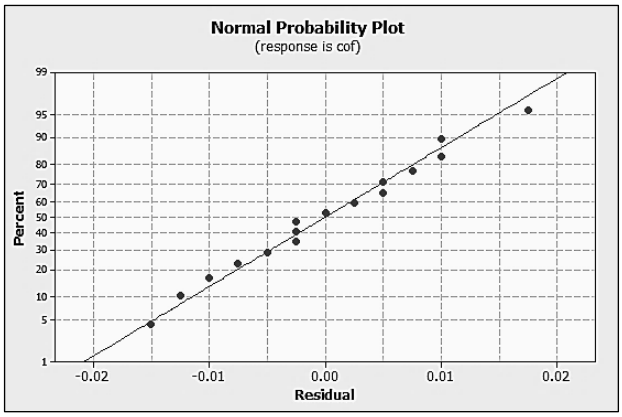

Fig. 8. Plot of residuals normal probability for sample friction coefficient.

Results from analysis leads to R^2 and its adjusted value, R^2(adj.) as 96.24% and 95.30% respectively for coefficient of friction as tabulated in Table 9. The suitability of the calculated constants is high as considerably good determination coefficient(R^2) to the tune of 0.9624 is obtained for coefficient of friction and hence the model is adequate to use for further analysis.

Table 9. Regression analysis for coefficient of friction of sample.

Terms	Coef	SE Coef	T	P
Constant	0.0225000	0.0110680	2.0329	0.065
Load	0.0043000	0.0002475	17.3746	0.000
Speed	0.0000450	0.0000247	1.8183	0.094
Temperature	-0.0001167	0.0000825	-1.4142	0.183
S=0.0110680	R^2 =96.24%		R^2(adj)=95.30%	

3.2.2.2 Analysis of variance for friction coefficient

ANOVA is used to analyze extent of input variables load, temperature, speed influence on friction coefficient characteristics of sample. The analysis is carried out at 5% level of significance. Table 10 shows analysis results for friction coefficient of sample.

Table 10. Results of ANOVA for friction coefficient of sample.

Source	DF	Adj SS	Adj MS	F-value	p-value	P%
Load(N)	3	0.03710	0.0123667	61.83	0.000	94.88
Speed (rpm)	3	0.00055	0.0001833	0.92	0.487	1.41
Temperature (°C)	3	0.00025	0.0000833	0.42	0.748	0.64
Error	6	0.00120	0.0002000			
Total	15	0.03910				

Load has maximum influence (94.88%) whereas other input factors speed (1.41%) and temperature (0.64%) have less influence on response variable, coefficient of friction.

3.2.3 Multi-Objective optimization

The set of parameters which results in near low wear and coefficient of friction is obtained through Taguchi methodology in combination with grey relation analysis, which is proven as effective method to solve multiple-objective optimization challenges. Normalized value of obtained friction coefficient and wear from experiment, values of grey relation coefficient along with grey relation grade and rank of experimental runs carried out are listed in table 11 below.

The Grey Relational Coefficient (GRC) which can be determined as

$$\zeta_i(k) = \frac{\Delta_{min} + \zeta\Delta_{max}}{\Delta_i(k) + \zeta\Delta_{max}}$$

Where $\Delta_i(k)$ is deviation sequence which is difference in absolute value between reference sequence($x_0^*(k)$) and comparability sequence ($x_i^*(k)$), Δ_{min} and Δ_{max} are the minimum and maximum values of the deviation sequence, ζ is Distinguishing or Identification coefficient and in general taken as 0.5.

Final step is to determine the gray relational grade (γ)

$$\gamma_{i=\frac{1}{n}\sum_{k=1}^{n}\varsigma_i(k)}$$

Where n denotes the number of experiments. The normalized values of response variables, calculated gray relational coefficients and grey relational grades are tabulated in Table 11. Rank is assigned based on the values of grey relational grade and the experiment with highest value of GRG is assigned rank 1 and close to be the optimum parameter combination among considered combinations.

The response table 12 shows that the load is dominant factor for achieving minimum rate of wear and minimum friction coefficient compared to speed and temperature.

Table 11. Normalized values, GRC, GRG, rank of experiment test runs.

Expt. Run	Normalized values of response variables		Grey relational coefficient (GRC)		Grey Relational Grade	Rank
	Wear	CoF	Wear	CoF		
1	1	0.875	1	0.8	0.9	1
2	0.919455	0.8125	0.861259	0.727273	0.794266	4
3	0.939591	0.9375	0.892206	0.888889	0.890547	3
4	0.870198	1	0.793901	1	0.89695	2
5	0.796468	0.6875	0.7107	0.615385	0.663042	5
6	0.704771	0.625	0.62875	0.571429	0.600089	7
7	0.739157	0.5	0.657166	0.5	0.578583	8
8	0.798637	0.5625	0.712898	0.533333	0.623115	6
9	0.515799	0.4375	0.508026	0.470588	0.489307	9
10	0.501859	0.375	0.500931	0.444444	0.472688	11
11	0.568154	0.3125	0.536569	0.421053	0.478811	10
12	0.446406	0.25	0.474566	0.4	0.437283	12
13	0.266109	0.1875	0.405222	0.380952	0.393087	13
14	0.152726	0.0625	0.37112	0.347826	0.359473	15
15	0.111214	0.125	0.360027	0.363636	0.361832	14
16	0	0	0.333333	0.333333	0.333333	16

Table 12. Signal to noise response table of GRG.

Levels	Load(N)	Speed(rpm)	Temperature(°C)
1	-1.217	-4.701	-5.322
2	-4.217	-5.458	-5.396
3	-6.575	-5.247	-5.053
4	-8.842	-5.445	-5.079
Delta	7.625	0.757	0.343
Rank	1	2	3

The optimum combination of selected parameters from the chosen levels is determined from the mean table of grey relation grade as in table 13. The level of control factor whose GRG value is maximum is the optimum level for that particular factor.

Table 13. Mean table of GRG.

Levels	Load(N)	Speed(rpm)	Temperature(°C)
1	**0.8704**	**0.6114**	0.5781
2	0.6162	0.5566	0.5641
3	0.4695	0.5774	**0.5906**
4	0.3619	0.5727	0.5853
Delta	0.5085	0.0547	0.0265
Rank	1	2	3

The combination of 10 N load, 100 rpm speed and 90°Ctemperature is found to be optimum for low friction coefficient and rate of wear.

4. CONCLUSIONS

Ni-P-SiC coating is produced successfully on SS 304 samples by electroless coating. The characteristics of the obtained coating were analyzed using FESEM. friction and wear characteristics of Ni-P-SiC coated SS 304 samples is studied by performing friction and wear test for sixteen experiments set according to L16 orthogonal array. The influence of selected control factors, load, speed, temperature on response variable, wear and coefficient of friction is studied through the tests by varying the level of considered factors. Based on the experimental results obtained by performing on samples specimens, the conclusions are drawn:

1. Optimal process parameters (such as 10 N load, 100 rpm speed, 90°C temperature) are found by design of experiments for minimum rate of wear and friction coefficient on pin on disc tribometer by coupling Taguchi and gray relational grade analysis.
2. The most significant parameter is load as compared to speed, temperature. It is verified by S/N ratio, ANNOVA and Regression mathematical modelling.
3. Linear regression analysis is carried out to illustrate the correlation among wear and considered factors for study and also coefficient of friction and selected operating parameters.

4. As per ANOVA results, load is the most dominant factor and influences wear and also coefficient of friction characteristics of Ni-P-SiC coated SS 304 sample to significant extent.

REFERENCES

[1] D.T. Gawne, U. Ma, *Friction and wear of chromium and nickel coatings*, Wear, vol. 129, iss.1, pp. 123–142, 1989, doi: 10.1016/0043-1648(89)90284-6

[2] A. Ramalho, J.C. Miranda, *Friction and wear of electroless NiP and NiP + PTFE coatings*, Wear, vol. 259, iss. 7-12, pp. 828–834, 2005, doi: 10.1016/j.wear.2005.02.052

[3] S. Karthikeyan, P.A. Jeeva, N. Arivazhagan, V. Umasankar, K.N. Srinivasan, M. Paramasivam, *Wear, hardness and corrosion resistance characteristics of tungsten sulfide incorporated electroless Ni-P coatings*, Procedia Engineering, vol. 64, pp. 720–726, 2013, doi: 10.1016/j.proeng.2013.09.147

[4] L.Y. Wang, J.P. Tu, W.X. Chen, Y.C. Wang, X.K. Liu, C. Olk, D.H. Cheng, X.B. Zhang, *Friction and wear behavior of electroless Ni-based CNT composite coatings*, Wear, vol. 254, iss. 12, pp. 1289–1293, 2003, doi: 10.1016/S0043-1648(03)00171-6

[5] Z.H. Li, X.Q. Wang, M. Wang, F.F. Wang, H.L. Ge, *Preparation and tribological properties of the carbon nanotubes-Ni-P composite coating*, Tribology International, vol. 39, iss. 9, pp. 953–957, 2006, doi: 10.1016/j.triboint.2005.10.001

[6] H. Ashassi-Sorkhabi, M. Es'haghi, *Corrosion resistance enhancement of electroless Ni-P coating by incorporation of ultrasonically dispersed diamond nanoparticles*, Corrosion Science, vol. 77, pp. 185–193, 2013, doi: 10.1016/j.corsci.2013.07.046

[7] E. Georgiza, V. Gouda, P. Vassiliou, *Production and properties of composite electroless Ni-B-SiC coatings*, Surface and Coatings Technology, vol. 325, pp. 46–51, 2017, doi: 10.1016/j.surfcoat.2017.06.019

[8] S. Zhang, K. Han, L. Cheng, *The effect of SiC particles added in electroless Ni-P plating solution on the properties of composite coatings*, Surface and Coatings Technology, vol. 202, iss. 12, pp. 2807–2812, 2008, doi: 10.1016/j.surfcoat.2007.10.015

[9] P.M. Gopal, K. Soorya Prakash, S. Nagaraja, N.K. Aravinth, *Effect of weight fraction and particle size of CRT glass on the tribological behaviour of Mg-CRT-BN hybrid composites*, Tribology International, vol. 116, pp. 338–350, 2017, doi: 10.1016/j.triboint.2017.07.025

[10] M.H. Cho, S. Bahadur, J.W. Anderegg, *Design of experiments approach to the study of tribological performance of Cu-concentrate-filled PPS composites*, Tribology International, vol. 39, iss. 3, pp. 1436–1446, 2006, doi: 10.1016/j.triboint.2006.01.012

[11] S.Y. Gajjal, A.J. Unkule, P.S. Gajjal, *Taguchi Technique for Dry Sliding Wear Behavior of PEEK Composite Materials*, Materials Today: Proceedings, vol. 5, iss. 1, pp. 950–957, 2008, doi: 10.1016/j.matpr.2017.11.170

[12] V.J. Banker, J.M. Mistry, M.R. Thakor, B.H. Upadhyay, *Wear Behavior in Dry Sliding of Inconel 600 Alloy using Taguchi Method and Regression Analysis*, Procedia Technology, vol. 23, pp. 383–390, 2016, doi: 10.1016/j.protcy.2016.03.041

[13] J.U. Prakash, S. Ananth, G. Sivakumar, T.V. Moorthy, *Multi-Objective Optimization of Wear Parameters for Aluminium Matrix Composites (413 / B 4 C) using Grey Relational Analysis*, Material Today Proceeding, vol. 5, iss. 2, pp. 7207–7216, 2018, doi: 10.1016/j.matpr.2017.11.387

[14] M. Fathi, M. Saman, S. Mahdavi, and S. Mirzazadeh, *Tribology International Co – P alloy matrix composite deposits reinforced by nano-MoS 2 solid lubricant: An alternative tribological coating to hard chromium coatings*, Tribology International, vol. 159, pp. 106-956, 2021, doi: 10.1016/j.triboint.2021.106956

[15] M. Czagány, P. Baumli, *Effect of surfactants on the behavior of the Ni-P bath and on the formation of electroless Ni-P-TiC composite coatings*, Surface and Coatings Technology, vol. 361, pp. 42–49, 2019, doi: 10.1016/j.surfcoat.2019.01.046

[16] A. Raza, K. Rana, Z. Farhat, *Preparation and tribological characterization of graphene incorporated electroless Ni-P composite coatings*, Surface and Coatings Technology, vol. 369, pp. 334–346, 2019, doi: 10.1016/j.surfcoat.2019.04.043

[17] D. Ram, G. Gyawali, Y.K. Kshetri, J. Choi, S. Wohn, *Microstructural and electrochemical corrosion properties of electroless Ni-P- TaC composite coating*, Surface and Coatings Technology, vol. 381, pp. 125-135, 2020, doi: 10.1016/j.surfcoat.2019.125135

[18] M. S. Safavi, M. Fathi, V. Charkhesht, M. Jafarpour, I. Ahadzadeh, *Electrodeposition of Co-P Coatings Reinforced by MoS 2 + Y 2 O 3 Hybrid Ceramic Nanoparticles for Corrosion-Resistant Applications: Influences of Operational Parameters*, Metallurgical and Materials Transactions A, vol. 51, pp. 6740–6758, 2020, doi: 10.1007/s11661-020-05987-8

[19] I. Ahmed, A. Ahmad, S. A. Rahaman, A. Abdul-rani, M. Azad, *Modelling and optimization of microhardness of electroless Ni-P-TiO2 composite coating based on machine learning approaches and RSM*, Journal of Materials Research and Technology, vol. 12, pp. 1010–1025, 2021, doi: 10.1016/j.jmrt.2021.03.063

[20] M.S. Safavi, A. Rasooli, F.A. Sorkhabi, *Coatings Electrodeposition of Ni-P / Ni-Co-Al 2 O 3 duplex nanocomposite coatings: towards improved mechanical and corrosion properties*, Transactions of the IMF, The International Journal of Surface Engineering and Coating, vol. 98, iss. 1, pp. 1–9, 2020, doi: 10.1080/00202967.2020.1802106

[21] A. Rasooli, M. Saman, S. Ahmadiyeh, A. Jalali, *Evaluation of TiO 2 Nanoparticles Concentration and Applied Current Density Role in Determination of Microstructural, Mechanical, and Corrosion Properties of Ni – Co Alloy Coatings*, Protection of Metals and Physical Chemistry of Surfaces, vol. 56, pp. 320–327, 2020, doi: 10.1134/S2070205120020215

[22] S. Kumar, R. Goli, S.K. Ghosh, *Performance analysis of SiC-Ni-P nanocomposite electroless coated brake pad*, Materials and Manufacturing Processes, vol. 37, iss. 7, pp. 1–18, 2021, doi: 10.1080/10426914.2021.1981932

[23] S. Kumar, S.K. Ghosh, *Porosity and tribological performance analysis on new developed metal matrix composite for brake pad materials*, Journal of Manufacturing Process, vol. 59, pp. 186-204, 2020, doi: 10.1016/j.jmapro.2020.09.053

[24] S. Kumar, Priyadarshan, S.K. Ghosh, *Statistical and computational analysis of an environment-friendly MWCNT/NiSO4 composite materials*, Journal of Manufacturing Process, vol. 66, pp. 11–26, 2021, doi: 10.1016/j.jmapro.2021.04.001

[25] S. Kumar, Priyadarshan, S.K. Ghosh, *Statistical and artificial neural network technique for prediction of performance in AlSi10Mg-MWCNT based composite materials*, Materials Cnemistry and Physics, vol. 273, pp. 125-136, 2021, doi: 10.1016/j.matchemphys.2021.125136

[26] S. Kumar, Priyadarshan, S.K. Ghosh, *Comparative Study of Airborne Particles on New Developed Metal Matrix Composite and Commercial Brake Pad Materials with ANN and Finite Element Analysis*, Computational Particle Mechanics, vol. 273, pp. 125-136, 2022, doi: 10.1007/s40571-022-00491-9

[27] S. Kumar, S.K. Ghosh, *Particle emission of organic brake pad material: A review*, Journal of Automobile Engineering, vol. 234, iss. 5, pp. 1213-1223, 2019, doi: 10.1177/0954407019879839

[28] S. Kumar, A. Mukhopadhyay, *Effect of Microstructure on the Wear Behaviour of Heat Treated SS- 304 Stainless Steel*, Tribology in Industry, vol 38, no. 4, pp. 445-453, 2016.